Journal of Alloys and Compounds xxx (2014) xxx–xxx

Contents lists available at ScienceDirect

Journal of Alloys and Compounds

journal homepage: www.elsevier.com/locate/jalcom

Influence of Cold Gas Spray process conditions on the microstructure of Fe-based amorphous coatings

J. Henao, A. Concustell *, I.G. Cano, N. Cinca, S. Dosta, J.M. Guilemany

Thermal Spray Centre, CPT, Universitat de Barcelona, 08028, Spain

ARTICLE INFO

Article history:
Received 31 July 2014
Received in revised form 1 November 2014
Accepted 5 November 2014
Available online xxxx

Keywords:
Metallic glass
Coatings
Cold Gas Spray
Microstructure

ABSTRACT

Fe-based amorphous metallic coatings were prepared by Cold Gas Spray process. Through this study, the effects of the process conditions such as spraying distance, gas pressure and temperature on the microstructure of as-sprayed coatings are evaluated. Microstructural studies show that the coatings can present a densely layered structure with porosity below 0.5% and thickness around 800 μm depending on the process conditions. Precipitation of nanocrystals in as-sprayed coatings is observed and present results show its dependence on the thermal and kinetic energy implicated in the process. In general, when gas temperature and pressure decreased, in the studied range, coatings displayed a dense and amorphous structure.

1. Introduction

Amorphous metals are produced by rapid quenching techniques (>10^3 K/s), retaining a short-range ordered structure (glassy structure). In particular, Fe-based metallic glasses (MG) present excellent soft-magnetic properties, wear and corrosion resistance and relatively low cost [1–7]. However, monolithic metallic glasses show little plasticity in compression and no ductility, hampering their industrial application. Thermal sprayed coatings from amorphous metals have raised increasing attention as an alternative to overcome their intrinsic brittleness while taking advantage of their outstanding properties.

The lack of grain boundaries, the weak points of crystalline materials, leads to a better resistance to wear and corrosion [7]. In addition, the amorphous alloys tend to have a low coercivity because there is no magnetocrystalline anisotropy. Furthermore, while metallic glasses are electrically conductive, the resistance to current flow is generally larger than that of the crystalline alloys. This helps to minimize current losses that occur due to the rapid magnetization and demagnetization of the material [7,8]. These properties make metallic glasses interesting within the surface engineering to protect structural materials and to create new functional hybrid materials.

Traditional thermal spray techniques use high thermal energy to produce coatings, which is a major drawback in order to preserve amorphous structure of the MGs. In last decades, researchers have been using different thermal spray techniques such as High Velocity Oxy-Fuel (HVOF), Flame Spray (FS) and Plasma Spray for obtaining amorphous coatings [9–13]. Several authors have reported crystallization and oxidation in amorphous coatings when HVOF, FS and Plasma Spray are used [10,13–18]. Crystallization and oxidation do not only affect the magnetic properties, but also mechanical properties of obtained coatings. For example, Liu et al. [19] found an increase in microhardness and a decrease in wear resistance when the degree of crystallization was higher in Fe-based coatings. On the other hand, Cold Gas Spray (CGS) process has arisen as alternative to the traditional thermal spray process [20]. CGS uses kinetic energy to deposit coatings through solid-state plastic deformation of micrometer scaled particles generating high strain rate (10^7–10^9 s^{-1}) at impact [21]. In CGS, impact particle conditions are critical to the final properties of the coatings because impacting particles need to achieve sufficient kinetic energy to reach intimate contact with the substrate to deform plastically upon impact [22].

Previous works have been carried out studying the impact behavior of particles in CGS. Parameters promoting high velocity and high temperature of the particles as well as preheated substrates are known to favor flattening, low coating porosity and high deposition efficiency [23–25]. Most of those works have been performed using crystalline materials such as Aluminum, Copper and Nickel alloys. In crystalline materials adiabatic shear instabilities in the particle/substrate interface have been suggested as the cause for bonding of particles in CGS [26]. Shear instabilities take place when the impact velocity of the sprayed particle exceeds a critical limit, producing a local heating that result in

* Corresponding author.
E-mail address: aconcustell@cptub.eu (A. Concustell).

http://dx.doi.org/10.1016/j.jallcom.2014.11.037
0925-8388/

excessive softening of the material. Subsequent fast cooling results in intimate bonding of the particle to the substrate.

However, the type of deformation in MGs is largely dependent on temperature and strain rate [5]. At high temperatures and low strain rates, homogeneous flow is promoted, so each volume element of the material contributes to the strain, resulting in uniform deformation for a uniformly stressed specimen. On the other hand, at low temperatures and high strain rates flow is localized in discrete thin shear bands (10 nm in the case of metallic glasses) keeping the rest of the material plastically undeformed, i.e. inhomogeneous flow. In previous studies, metallic glasses have been deposited by CGS using a pre-heating system for the amorphous particles and helium as carrier gas, resulting in low crystallization and absence of oxidation [14,21].

This paper focuses on the deposition characteristics and its effect on the microstructure of Fe-based coatings in order to optimize the final properties of coatings in CGS process. Different stand-off distances, gas pressures and temperatures were used in the experiments. Densification and low crystallization was reached at low gas pressure and temperature conditions in the studied range.

2. Experimental procedure

The Fe-based amorphous powder (Trademark "KUAMET®6B2", Epson-Atmix Corp., Hachinohe-shi, Aomori, Japan) was manufactured using water atomization (SWAP®). This powder was sieved to −40 + 20 μm before spraying. Particle size distribution was determined by means of a laser diffraction equipment (LS 13 320 Laser Diffraction, Beckman Coulter, Inc., 250 S. Kraemer Blvd, Brea, CA) Characterization of the powder was conducted using a scanning electron microscopy (SEM) (Jeol JSM 5310, JEOL, Inc., Peabody, MA) to reveal the powder morphology. X-ray diffraction (XRD) was carried out in a Diffractometer of powders (PANalytical X'Pert PRO MPD, PANalytical, Almelo, Netherlands) to check the amorphous structure of the feedstock powder. A differential scanning calorimeter (DSC-1, Mettler-Toledo S.A.E, Barcelona, Spain) was used to measure characteristic temperatures of the alloy, the glass transition temperature (T_g) and the crystallization temperature (T_x). Samples were introduced into Al pans and then loaded into the DSC apparatus. After temperature equilibration, powder specimen was continuously heated up at (0.167 K s^{-1}) to 873 K, above full crystallization temperature. Characteristic temperatures were measured from DSC curves by following the ASTM E1356 Standard.

A commercial equipment of Cold Gas Spray system Impact Spray 5/11 (Impact Innovations, Ampfing, Germany) was used to deposit coatings onto several mild steel substrates with a flat geometry (100 × 50 × 5 mm). These were prepared by grinding using 240 grit SiC paper. The cold spray equipment allowed changing the main parameters of the process working with a maximum operating temperature of 1000 °C and pressure of 50 bar. Three spraying distances (10, 30 and 50 mm), two pressures (40 and 50 bar) and two temperatures (900 and 1000 °C) were tested. Process parameters are listed in Table 1. Other parameters were kept constant such as type of gas (N_2), powder feeding rate and the gun travel speed (250 mm/s). Normalized deposition efficiency of the process was calculated by measuring the increment of mass of the substrate after deposition and normalizing by the mass of the coating with higher weight.

Cross-sectional microstructures of the as-sprayed coatings were investigated by means of an optical microscope (OM) (Leica DMI 5000 M, Leica microsystems, GmbH). Porosity was measured (ASTM E2109-01 standard) using the image analysis software Image J [21]. Coatings were also characterized by SEM and their amorphous structure checked by XRD using a D/max 2400 X-ray diffractometer (PANalytical, Almelo, Netherlands) equipped with a monochromatic Cu Kα X-ray source (λ = 1.54056 Å; 40 kV; 100 mA). XRD patterns were collected in the range of 30° < 2θ < 100° at the step size of 0.02°. Vickers hardness tests were performed in a micro-Vickers indenter (Matsuzawa indenter MXT CX-1, Matsuzawa Co., Ltd, Akita-shi, Akita, Japan) with a load of 300 gF and dwell time of 10 s were also performed to identify the optimum coatings obtained from the experimented spraying parameters. At least, 10 indentations were collected on the polished cross-sectional surface of each coating specimen.

Table 1
Process parameters for the different series studied.

Spraying conditions	Process gas		Stand-off distance (mm)
	Pressure (bar)	Temperature (°C)	
1, 2 and 3	40	900	10, 30, 50
4, 5 and 6	50	900	10, 30, 50
7, 8 and 9	40	1000	10, 30, 50
10, 11 and 12	50	1000	10, 30, 50

3. Results and discussion

3.1. Feedstock material

Characteristics of the Fe-base amorphous powders used as feedstock material are displayed in Fig. 1a. Spherical particles having a smooth surface are typical from the gas atomization process. The distribution profile got from LS measurement of the powders shows a micrometric particle size varying from 5 μm to 100 μm and an average particle size of 30 μm. XRD analysis of the powder is shown in Fig. 1b, the diffuse peak in the pattern is characteristic for an amorphous material. DSC measurements shown in Fig. 1c revealed an endothermic heat flux corresponding to the glass transition at 476 °C (T_g) and an exothermic peak due to crystallization

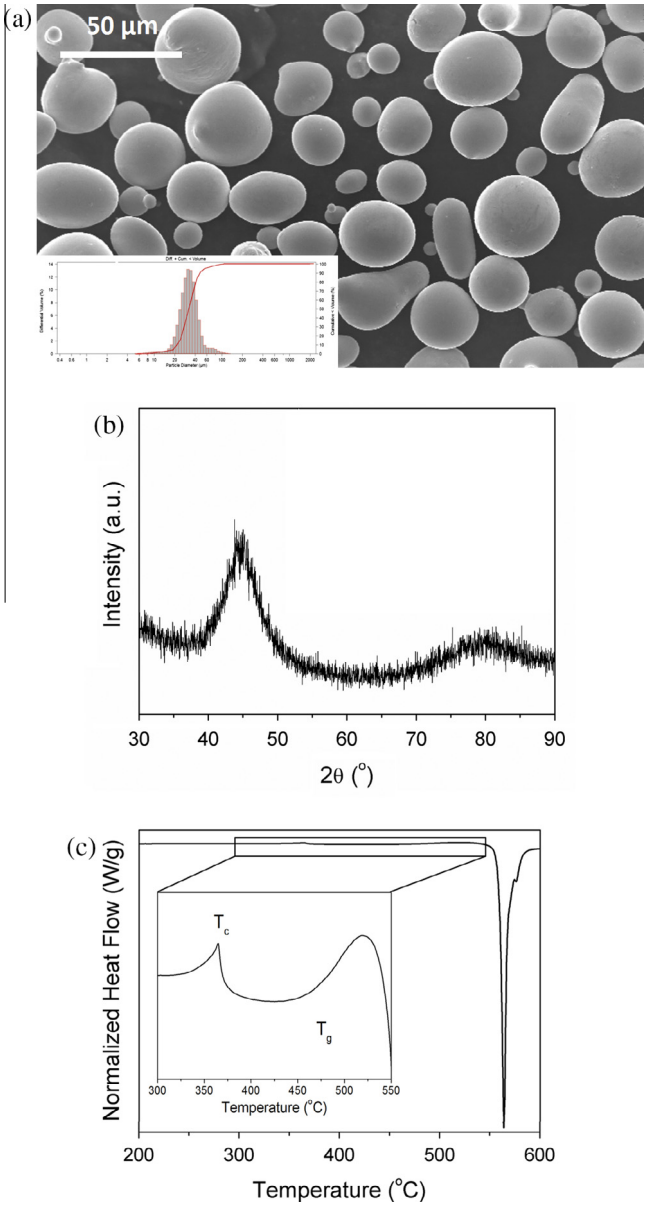

Fig. 1. Characteristics of as-atomized Fe-based amorphous powders. (a) Surface morphology and size particle distribution, (b) XRD patterns and (c) DSC scans of the Fe-based amorphous powder.

of the supercooled liquid at 561 °C (T_x). The inset shows thermal relaxation of the studied alloy and the Curie temperature (T_c) is also clearly visible.

3.2. Efficiency of CGS process

Efficiency of the CGS process greatly depends on the process parameters. Fig. 2 shows the normalized efficiency depending on the different spraying parameters. Efficiency decreases at higher gas pressure but also at higher gas temperature in the studied range. Therefore, higher particle velocity does not improve efficiency of the process for this material. Metallic glasses change their deformation behavior depending on the temperature and strain rate. In fact, high strain rates promote inhomogeneous flow (i.e. brittle behavior) even at temperatures above the glass transition as shown in Ref. [22]. It is feasible then, that increasing particle velocity, deformation mode of particles changes from homogeneous/plastic flow to inhomogeneous/localized flow.

3.3. Gas pressure influence

In Cold Gas Spray process, the powder feedstock is accelerated by the momentum transfer from the gas dynamics. The thermal energy and pressure of the processing gas provide the kinetic energy to the particles for the impact onto the substrate. Particles during the impact undergo a shear rate of 10^7–10^9 s^{-1} [14]. The plastic deformation of particles causes the formation of coating onto the substrate. Fig. 3a and b shows cross-sectional structure of the as-sprayed coatings at the same gas temperature (900 °C) but at lowest gas pressure and highest gas pressure, respectively. In general, coatings have high thickness around 800 μm when spraying conditions were fixed at low gas pressure (40 bar), Fig. 3c. A dense structure with porosity below 0.5% is noticed in Fig. 3a at the best spraying conditions, showing that particles deformed homogeneously upon impact.

As it has been mentioned in previous section, efficiency of the process decreases at higher gas pressure while keeping temperature constant at 900 °C. This is reflected in the results displayed in Fig. 3c, with higher porosity and lower thickness at higher pressure. However, deposition efficiency increases at the same high pressure, once gas temperature is 1000 °C. In Cold Gas Spray, the impact behavior largely depends on factors such as material properties of the feedstock powders, type of substrate and spraying parameters [20,27]. In this work, coating formation depends on gas pressure, but present results also show a low correlation between deposition efficiency, porosity and thickness on gas pressure. It is interesting to note that gas pressure is directly related to the kinetic energy of the process imparting higher velocities to the particles at impact because acceleration of particles scales with the density of the process gas, increasing with higher pressure [28]. Efficiency, porosity and thickness results suggest that the particles are rejected from the surface upon impact at higher gas pressure. This effect may be due to reduced residence time of particles in the jet and higher impact velocity which change conditions of deformation and critical impact velocity.

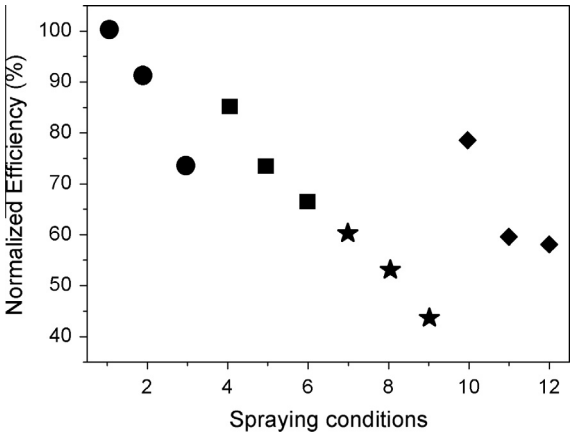

Fig. 2. Normalized efficiency depending on the different spraying parameters.

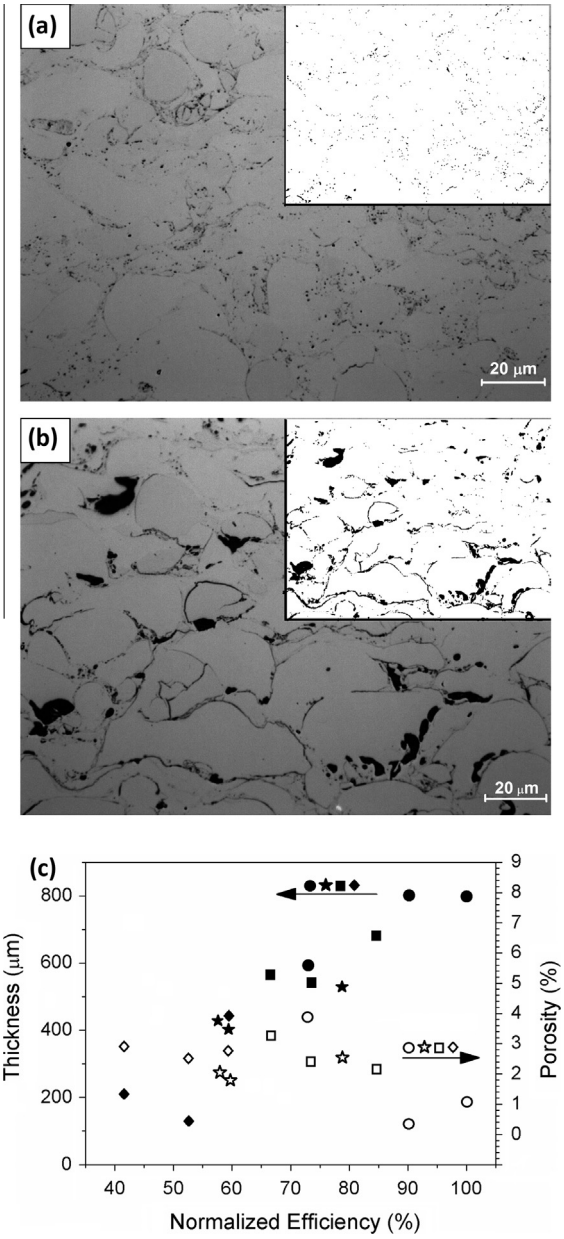

Fig. 3. (a and b) Cross-sectional structure of the as-sprayed coatings at the same gas temperature but at lowest gas pressure and highest gas pressure, respectively. (c) Normalized efficiency-thickness and porosity of as-sprayed coatings under different spraying conditions.

3.4. Stand-off distance influence

Fe-based coatings were also obtained using different spraying distances. This allowed studying the effect of the spraying distance in the morphology of the coatings. Fig. 2 shows that, independently of the gas temperature and pressure, normalized efficiency decreases as stand-off distance increases.

There was a marked difference in the density of coatings when the spraying distance was 50 mm showing large voids between particles. By contrast, small pores were identified when the spraying distance was 10 mm decreasing the value of porosity around 0.5%, see Fig. 3c. When the spraying distance was 10 mm, as shown in Fig. 3c, coatings presented higher values of thickness than at 50 mm. Both results, porosity and thickness are related to the effect of the in-flight particle time. At short stand-off distance, the reduced in-flight particle time until impact on the substrate resulted in a decrease of porosity and an increase of efficiency for a given kinetic energy (process at constant gas temperature and pressure). The effect of different gas temperature on amorphous coatings formation by CGS was studied by Yoon et al. [21]. They observed defective microstructures, such as pores and splat boundaries, and decreased their presence by an increase in the thermal energy, particle temperature, at impact. From the present work, it is suggested that particles lose temperature and increase velocity when they had longer in-flight time before the impacting the substrate, in agreement with literature [20].

3.5. Gas temperature influence

The influence of gas temperature on coating formation was also studied in this work. As shown in Fig. 3, process efficiency and properties of coatings were poorer when the spraying gas temperature was higher (1000 °C). Thickness decreased and porosity increased for both spraying distances. Microstructure of the coatings was also investigated by XRD and DSC. Fig. 4 shows XRD patterns of feedstock powder, (a), and as-sprayed coatings using both gas temperature of 900 °C, (b and c), and 1000 °C (d and e). These patterns revealed the amorphous structure in the feedstock powder; however some crystallization occurred during the CGS process. The crystallized volume fraction was evaluated by DSC and Fig. 5 shows V_{crys} versus process efficiency. Interestingly, process efficiency increases when crystallization is avoided.

Gas temperature in the CGS process contributes into the acceleration of the particles by governing the expansion of the gas into supersonic flow in the convergent–divergent nozzle, but also, to the heating of the particles in-flight. It has been shown that increasing particle temperature is useful in improving coating density and process efficiency in crystalline materials [20]. In the case of amorphous metallic systems, several authors have studied the effect of temperature in the deformation behavior of amorphous metallic materials [5,29,30]. The effect of increasing material temperature close and above T_g causes thermal softening allowing metallic glasses to show homogeneous deformation. Homogeneous deformation of amorphous powder would allow coating built-up,

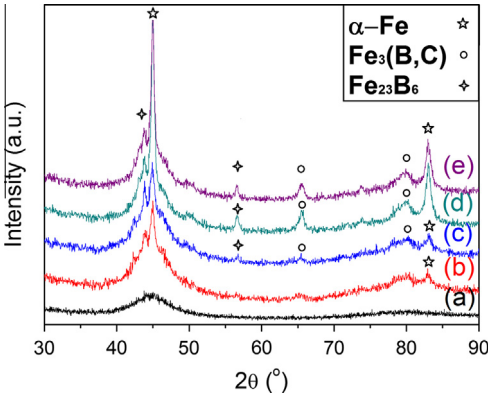

Fig. 4. X-ray diffraction pattern of the amorphous powder (a), coatings built-up at standoff distance of 30 mm and T_{gas} = 900 °C: P_{gas} = 40 bar (b), T_{gas} = 900 °C: P_{gas} = 50 bar (c), T_{gas} = 1000 °C: P_{gas} = 40 bar (d) and T_{gas} = 900 °C: P_{gas} = 40 bar (e).

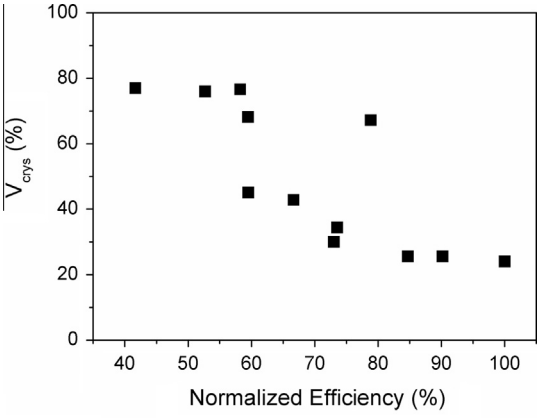

Fig. 5. Plot of V_{crys} versus process efficiency.

showing high deposition efficiency. Up to now, most works related to CGS deposition of metallic glasses refer to this phenomenon occurring when particle temperature achieves a temperature between T_g and T_x. However, increasing gas temperature also results in higher velocity of particles and higher strain rates during impact, which could favor inhomogeneous deformation in metallic glasses [5]. Finally, it is remarkably certain that metallic glasses at temperatures between T_g and T_x deform inhomogeneously at typical impact strain rates in CGS [29]. Therefore, it is not clear that increasing gas temperature in metallic glass deposition results in increased efficiency, as shown in the present work.

Crystallization presented in the as-sprayed coatings in this work could be caused due to the high temperature experienced by the in-flight particles. Gas temperature of 900–1000 °C could contribute to overcome the activation energy for crystallization. In addition, some authors attribute crystallization of the amorphous metallic particles in the Cold Gas Spray process to the high strain rate experimented by the particles upon the impact [31]. Nucleation and growth of crystalline structures in amorphous alloys require local and long range atomic diffusion. The extremely short impact time (10^{-8} s) in Cold Gas Spray process limits long-range atomic diffusion and may only generate the formation of nanocrystals in some localized areas [31] in agreement with XRD patterns shown in Fig. 4. However, the study of the origin of crystallization in the Fe-based as-sprayed coatings will be studied in future research and goes beyond of the scope in this work.

In the range of conditions used in this study, the optimum conditions for the formation of metallic glass coatings are those favoring lower impact velocities, i.e. lower strain rates, and higher particle temperatures, i.e. lower stand-off distance, thus promoting conditions of homogeneous flow in the impacting particles.

3.6. Mechanical properties

In order to verify the mechanical properties of the obtained amorphous metallic coatings, the Vickers microhardness was measured. Vickers microhardness decreased with lower normalized efficiency as is shown in Fig. 6. This result was expected due to the higher porosity presented in coatings with lower deposition efficiency, i.e. higher gas temperature and pressure and higher stand-off distance. The poor contact between particles and voids in these coatings act as stress concentration sites decreasing the resistance to the penetration. However, coatings still remain having higher microhardness values compared with other materials used in the industry such as bearing steel (200 Hv) [29]. It is interesting to note that nanocrystallization produced in different spraying conditions results in harder coatings. Concustell et al. [32] also

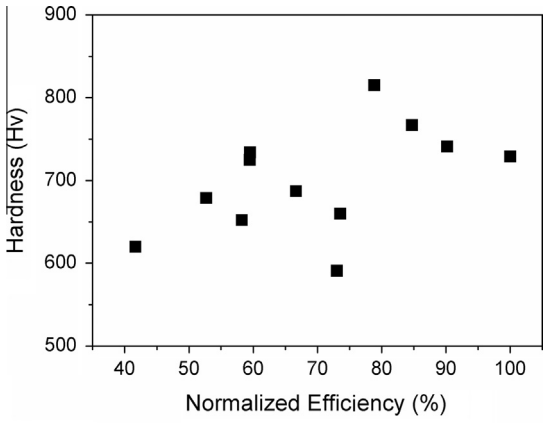

Fig. 6. Vickers micro-hardness in function of the normalized deposition efficiency.

found that precipitation of nanocrystals in Cu-base metallic glasses was an effective measure to increase microhardness, yield strength and elastic modulus. However, it was also found increased brittleness due to higher structural relaxation of the amorphous matrix.

4. Conclusions

Cold Gas Spray process can be established as a suitable technique to produce metallic amorphous coatings controlling the main spraying parameters of the process. In this work, Fe-based amorphous metallic glass was deposited using Cold Gas Spray process onto mild-steel substrates. The as-sprayed coatings obtained exhibits high density, thickness and Vickers microhardness when process conditions were optimal. Moreover, the as-sprayed coatings retained the amorphous structure of the feedstock material with low degree of crystallization.

It was found that parameters such as spraying distance, gas pressure and gas temperature affects conditions of particles deformation during the impact. Conditions using low values of gas pressure, spraying distance and gas temperature results optimal to produce dense coatings. At these conditions particles reach the surface at high temperature and high velocity, leading to high deposition efficiency and low porosity. Low particle temperature at impact due to higher stand-off distance results in lower deposition efficiency. Higher gas temperature and pressure also results in lower deposition efficiency probably due to two possible effects: inhomogeneous flow of the particles during impact and/or crystallization in-flight or during impact. Therefore, dense metallic glass coatings are formed when homogeneous flow is promoted during impact.

Acknowledgements

The authors would like to thank IMPACT INNOVATIONS GmbH for their collaboration in coating built-up. EPSON-ATMIX is also acknowledged for providing the feedstock powder used in this work. Finally, financial support from Generalitat de Catalunya through SGR 2009-390 is acknowledged.

References

[1] V. Keryvin, V.H. Hoang, J. Shen, Intermetallics 17 (2009) 211–217.
[2] A. Inoe, B.L. Shen, C.T. Chang, Acta Mater. 52 (2004) 4093–4099.
[3] S.J. Pang, T. Zhang, K. Asami, A. Inoue, Corros. Sci. 44 (2002) 1847–1856.
[4] A. Makino, T. Bitoh, A. Kojima, A. Inoe, T. Masumoto, J. Magn. Magn. Mater. 215–216 (2000) 288–292.
[5] M. Trexler, N. Thadhani, Progr. Mater. Sci. 55 (2010) 759–893.
[6] I. Kaban, P. Jovari, A. Waske, M. Stoica, J. Bednarcik, B. Beuneu, N. Mattern, J. Ecker, J. Alloys Comp. 586 (2014) S189–S193.
[7] W.H. Wang, C. Dong, C.H. Shek, Mater. Sci. Eng. R 44 (2004) 45–89.
[8] F.J. Loffer, Intermetallics 11 (2003) 529–540.
[9] H. Miura, S. Isa, K. Omuro, Trans. Jpn. Inst. Met. 25 (1984) 284.
[10] J. Voyer, Mater. Sci. For. 690–634 (2011) 405–408.
[11] X.Q. Liu, Y.G. Zheng, X.C. Chang, W.L. Hou, J.Q. Wang, Mater. Sci. For. 633–634 (2010) 685–694.
[12] C. Zhang, L. Liu, K.C. Chan, Q. Chen, C.Y. Tang, Intermetallics 29 (2012) 80–85.
[13] L. Liu, C. Zhang, Thin Solid Film, 15.08.13, http://dx.doi.org/10.1016/j.tsf.2013.08.029.
[14] H. Choi, S. Yoon, G. Kim, H. Jo, C. Lee, Scripta Mater. 53 (2005) 125–130.
[15] R.Q. Guo, C. Zhang, Q. Chen, Y. Yang, N. Li, L. Liu, Corros. Sci. 53 (2011) 2351–2356.
[16] J. Kim, C. Lee, H. Choi, H. Jo, H. Kim, Mater. Sci. Eng. A 449–451 (2007) 858–862.
[17] X.Q. Liu, Y.G. Zheng, X.C. Chang, W.L. Hou, J.Q. Wang, Z. Tang, A. Burgess, J. Alloys Comp. 484 (2009) 300–307.
[18] J.H. Choi, C. Lee, D.B. Lee, J. Alloys Comp. 449 (2008) 384–388.
[19] G. Liu, Y. An, J. Chen, G. Hou, J. Chen, Tribol. Lett. 46 (2012) 131–138.
[20] M. Villa, S. Dosta, J. Fernandez, J.M. Guilemany, Revista de Metalurgia 48 (3) (2012) 175–191.
[21] S. Yoon, H.J. Kim, C. Lee, Surf. Coat. Technol. 200 (2006) 6022–6029.
[22] http://rsbweb.nih.gov/ij/index.html.
[23] X.K. Wu, J. Zhang, X. Zhou, H. Cui, J. Liu, Sci. China Tech. Sci. 55 (February) (2012) 357–368.
[24] D. Goldbaum, R.R. Chromik, S. Yue, R. Irissou, J.G. Legoux, J. Thermal Spray Technol. 20 (3) (2011) 486–496.
[25] D. Goldbaum, J.M. Shockley, R.R. Chromik, A. Rezaeian, S. Yue, R. Irissou, J.G. Legoux, J. Thermal Spray Technol. 21 (2) (2012) 288–303.
[26] H. Assadi, F. Gartner, T. Stolenhoff, H. Kreye, K. Kang, Acta Mater. 51 (2003) 4379–4394.
[27] A.L. Greer, Y.Q. Cheng, E. Ma, Mater. Sci. Eng. R 74 (71) (2013) 71–132.
[28] H. Assadi, T. Schmidt, H. Richter, J.-O. Kliemann, K. Binder, F. Gärtner, T. Klassen, H. Krey, J. Thermal Spray 20 (2011) 1161.
[29] S. Yoon, H.J. Kim, G. Bae, B. Kim, C. Lee, J. Alloys Comp. 509 (2011) 347–353.
[30] S. Yoon, C. Lee, H. Choi, H. Kim, J. Bae, Mater. Sci. Eng. A449–451 (2007) 911–915.
[31] S. Yoon, G. Bae, Y. Xiong, S. Kumar, K. Kang, J.J. Kim, C. Lee, Acta Mater. 57 (2009) 6191–6199.
[32] A. Concustell, G. Alcala, S. Mato, T.G. Woodcock, A. Gebert, J. Eckert, M.D. Baró, Intermetallics 13 (2005) 1214–1219.